MODELING THE MARTIAN ATMOSPHERE WITH THE LMD GLOBAL CLIMATE MODEL. F. Forget[1], E. Millour[1], F. Gonzalez-Galindo[1], S. Lebonnois[1], J-B. Madeleine[1], P-Y. Meslin[1], L. Montabone[1,3], A. Spiga[1], F. Hourdin[1], F. Lefevre[2], F. Montmessin[2], S.R. Lewis[3], P. Read[4], M.A. Lopez-Valverde[5], G. Gilli[5]
[1]Laboratoire de Météorologie Dynamique, Université Paris 6, BP 99, 75005 Paris, FRANCE (forget@lmd.jussieu.fr) [2]Service d'Aeronomie, Paris, FRANCE, [3]The Open University, Milton Keynes, UK, AOPP, [4]University of Oxford, UK, [5]Instituto de Astrofisica de Andalucia, 18080 Granada, Spain..

Introduction: For several years we have been developing a 3D Global Climate Model (GCM) for Mars derived from the models used on Earth for weather forecasting or climate changes studies [1]. The purpose of such a project is ambitious: we wish to build a "Mars simulator" based only on physical equations, with no tailor-made forcing, but able to reproduce all the available observations of the Martian climate (temperatures, winds, but also clouds, dust, ices, chemical species, etc...).

The GCM is constantly evolving, thanks to a contnuous collaboration between several teams based in France (LMD, SA), the UK (The Open University, University of Oxford) and Spain (Instituto de Astrofisica de Andalucia), and with the support of ESA and CNES.

We are currently working on an improved version of the model. Several new parametrisation are included in the heart of the model (radiative transfer, surface and subsurface processes, dynamics) and the applications of the GCM are in contnuous development (Water, dust, CO2, radon cycles, photochemistry,thermosphere, ionosphere, etc...)

Simulating the thermal structure and cirulation: current design of the General Circulation Model and recent improvements.

A description of the basic version of the LMD-AOPP GCM can be found in [1]. We continue to use the 3.75° (latitude) x 5.625° (longitude) horizontal resolution for our baseline simulations, although 2°x2° or even "zoomed" simulations have been performed for specific studies. In the vertical, our first mid-layers are typically located near 5m, 20, 40, 100 m ... up to above 80 km (25 layers version), 120 km (32 layers version) or above 300 km (50 layers version).

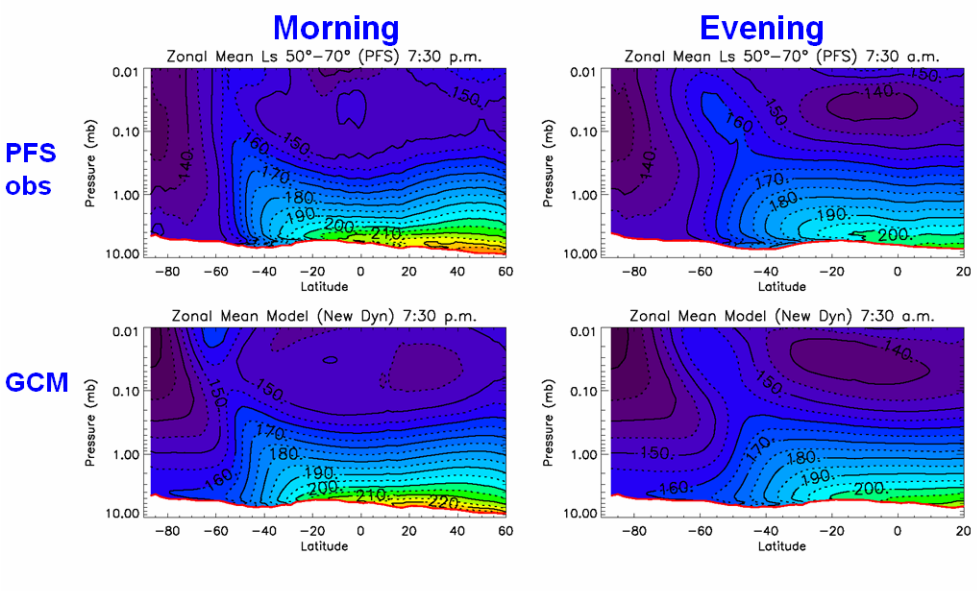

Figure 1: A comparison between Mars Express PFS observations (obtained at two different local times) with GCM predictions at the same location and time. Figure from Giuranna et al. [4].

In most cases, the current version of the GCM is able to reproduce the thermal structure of the atmosphere below 50km (where most of the observations are available) with good accuracy (e.g. Figure 1). Despite of the large diurnal, seasonal, and spatial variability of the Martian atmosphere, temperatures are usually within a few kelvins of the observations [2]. However, atmospheric temperatures primarily depend on the amount of dust in the atmosphere, which strongly varies in space and time, and of which the optical properties are not very well known.. To obtain realistic results in our baseline GCM, we still have to assume a prescribed "dust distribution scenario" derived from the available observations.

We have recently also developed an *improved radiative transfer code* to compute the dust heating at solar wavelength with more accuracy. This code is based on the always sucessful Toon et al. (1989) parameterisation [3]. It has been validated against specific Monte Carlo simulations. To better simulate radiative effect of dust in the atmosphere, we now take into account the possible variations of the dust size distribution. For this purpose, the single scaterring properties of aerosols can be calculated in each model box at each timestep.

In some locations, it appears that clouds may radiatively affect the thermal structure[5]. This had not been taken into account in our baseline GCM, but our new radiative transfer code combined with our ability to simulate Mars water ice clouds (see below) now allow us to take that into account [6]. In the past, we had reported that simulating the polar night thermal structure was a difficult problem. Indeed, our GCM predicted there atmospheric temperature significantly warmer than the available observations [4]. We have recently been able to solve this problem by improving the way the atmospheric mass was numerically updated at each timestep in our atmospheric "dynamical core". This improved model now simulate cold temperatures and CO2 condensation in the winter high latitudes (figure 2), and allows a sucessful simulation of the non-condensable gas enrichment in the polar night [7] put forward by the GRS spectrometer [8] and which has also been detected using Mars Express OMEGA when monitoring CO in Hellas Planitia [9].

Such an improved model will allow us to better simulate the energy balance of the polar regions and thus the *CO_2 condensation/sublimation cycle*. For this purpose, we continue to use the detailed scheme for CO2 ice condensation and sublimation in the polar caps described in [11]. A major recent improvement is the inclusion of the high thermal inertia subsurface water ice layer detected by Mars Odyssey which has been shown to strongly affect the energy balance (and thus the CO2 condensation rate) [12] (figure 3). This required the development of a new subsurface sheme in which the soil thermal properties (heat capacity, conductivity) could vary along the vertical. This improved model includes 18 layers with mid-levels starting at 0.2 mm below the surface (to capture the diurnal cycle in low thermal inertia regions), down to 18.5 m (to simulate the seasonal cycle in icy, high conductivity subsurface). We are now working with Mars Odyssey data to include a reference subsurface ice map in both polar regions [13]. Because the absolute depth of the ice is not perfectly known, however, we use a "ice depth parameter" to fit the Viking lander pressure curve and tune our CO2 cycle scheme.

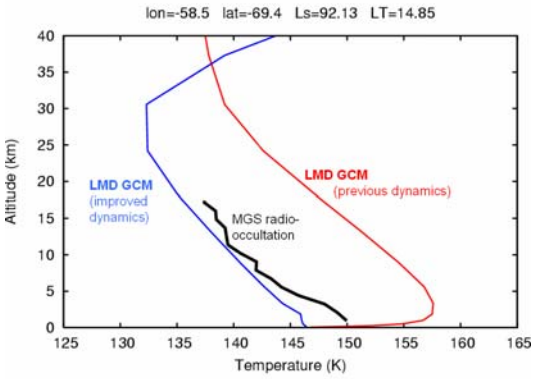

Figure 2: An example of comparison between a southern polar night Mars Global Surveyor radio-occultation [10] with prediction from the LMD GCM using the improved dynamical core.

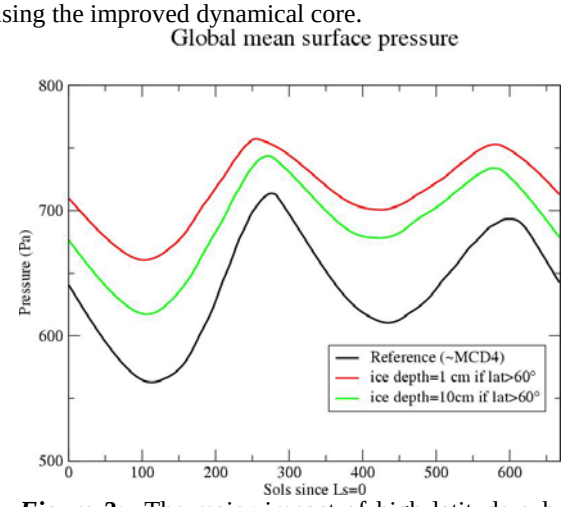

Figure 3: The major impact of high latitude subsurface ice on the CO2 cycle simulated by the GCM. This confirms the finding of [12]

Upper atmosphere and thermosphere

The GCM has been carefully extended to high altitude [14-16]. Above about 80 km, this required to take into account non-LTE radiative transfer in CO2 gas. Above 120 km, it was necessary to include all the processes that controls a thermosphere : Extreme UV heating, molecular conduction, molecular diffusion of most neutral species and key reactors, and complete photochemistry. The validation of the simulations of the upper atmosphere remains difficult. In fact, above 60 km on Mars, very little data is available. SPICAM on Mars Express has provided the first remote sensing observations of the thermal structure between 60 and 130 km [17]. Their analysis with the GCM suggest that the model significantly overestimate the temperatures most of the time around the mesopause (above 80 to 100 km), by up to 30 K, probably because of an underestimation of the atomic oxygen concentration which controls the CO2 infrared cooling at the level of the mesopause [17]. Generally speaking, NLTE CO2 cooling appears to be the key process controlling the thermal structure and the circulation of the high Martian atmosphere, and we are currently working on a much improved version of its parameterisation.

Comparisons have also been performed with wind measurements obtained around 50 to 90 km by monitoring the Doppler-shift in the microwave [18] and infrared [19] atmospheric emission, using Earth-based telescope. These measurements suggest that the simulated winds are often much weaker than in reality. Such observations may question our understanding of Mars upper atmosphere in the future.

A next step is the inclusion of the Ionosphere, to create one of the first 3D ionospheric model [20]

A key application: simulating the water cycle.

The GCM is used to simulate the current Mars water cycle and interpret the available observations. Our baseline water cycle includes 1) condensation and sublimation on and from the surface 2) water vapor and ice transport by the general circulation as well as mixing by turbulence and convection, 3) atmospheric water ice condensation and sublimation using simple cloud microphysics [21]. We are also currently working on an improved parametrisation of exchange with the sub-surface [22].

Initially, simulating the first order behavior of the water vapor, clouds and surface frost as observed by TES, PFS, OMEGA or SPICAM on the basis of physical equations had been found to be relatively easy [21]. Recently, the re-estimation of the water vapor columns (see [23]) has driven us to "tune" our water cycle model by slightly raising the frost albedoes and by modifying the cloud microphysics, to enhance the equivalent ice particle size in order to increase the ice particles sedimentation velocity.

Figure 5 illustrates the seasonal evolution of the zonal mean water vapor in comparison with the revised TES data provided by M. D. Smith (personal communication). The agreement is good. The slight overestimation in the tropics around Ls=360° is thought to reflect an overestimation of the atmospheric surface pressure (resulting from an imperfect CO2 cycle simulation) known for this season in this version of our GCM. The stronger disagreement observed in the southern high latitudes in summer (Ls=320°-360°) remains puzzling and deserves a specific investigation. The GCM also predicts some spatial variations in the distribution of water vapor, in qualitative agreement with the observations [23] (which exhibit structures which should not exist if water vapor is uniformly mixed). Our analysis shows that these structures have a purely dynamical origin, the local enhancement of water vapor resulting from a convergence of "humid" air combined with cloud sublimation. The clouds themselves are, to first order, predicted in good agreement with the TES and OMEGA observations. Their radiative effects are just starting to be taken into account in our GCM [6].

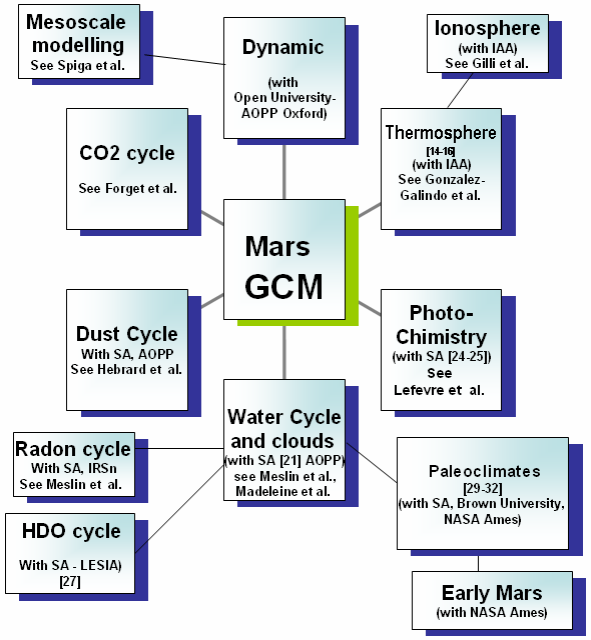

Figure 4 : A schematic list of the current scientific application of the GCM, illustrating collaboration with various institutes, suggesting link to other contributions to the workshop, along with key references.

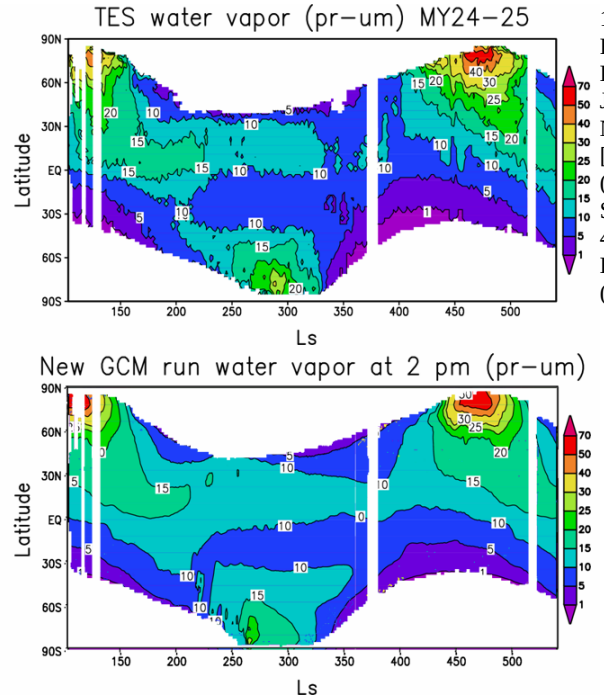

Figure 5 : Seasonal evolution of the zonal mean water vapor column at 2pm as observed by TES (revised values, M.D. Smith personal communication) in Martian Year 24-25 and predicted by the GCM. A mask is applied on the GCM data to mimic the observations and help the comparison.

Other applications of the GCM.

The model is now used as a "platform" to simulate many aspects of the Mars climate system : Photochemistry [24-26], dust cycle, deuterium cycle[27], exhalaison and transport of Radon [28]. It is also used to explore Mars past climates [29-32]. These applications are illustrated in Figure 4. Moreover the outputs of the GCM are available to the community through the Mars Climate Database, as described in [2]

References: [1] Forget et al. JGR. 104 , 24,155-24,176 (1999); Hourdin et al. JAS 50, 3625-3640, (1993) [2] Millour et al. This issue [3] Toon et al., JGR 94,16287-16301 (1989) [4] Giuranna et al., Icarus, in press (2008) [5] Wilson et al., GRL 35-7 (2008) [6] Madeleine et al., this issue [7] Forget et al., this issue [8] Sprague et al., Science 306, Issue 5700, pp. 1364-1367 (2004) [9] Encrenaz et al., A&A 459, 265-270 (2006) [10] Hinson et al. JGR 104, E11, p. 26,997 (1999). [11] Forget et al., Icarus 131, 302-316, (1998) [12] Haberle et al., PSS 56, 2, p. 251-255 (2008) [13] Diez et al. Icarus196-2, p. 409-421 (2008) [14] Angelats i Coll, GRL 32, 4 (2005) [15] Gonzalez-Galindo et al. JGR 110, CiteID E09008 (2005) [16] Gonzalez-Galindo et al., this issue [17] Forget et al., JGR, in press, 2008 [18] Moreno et al., submitted to Icarus, 2008 [19] Sonnabend, Sornig et al., this issue [20] Giili et al., this issue [21] Montmessin et al., JGR 109, Issue E10 (2004) [22] Meslin et al., this issue [23] Fouchet et al. Icarus 190, Issue 1, p. 32-49 (2007) [24] Lefevre et al. JGR 109, Issue E7 (2004); Lebonnois et al., JGR 110, E3, CiteID E03006, (2005) [25] Lefevre et al., Nature 454, 971.(2008) [26] Lefevre and Forget, this issue [27] Montmessin et al. JGR 110, Issue E3, CiteID E03006 (2005) [28] Meslin et al., this issue [29] Forget et al., Science, 311 pp. 368-371 (2006) [30] Levrard et al. Nature, 431 (2004). [31] Montmessin et al. JGR 112, E8, CiteID E08S17 (2007) [32] Madeleine et al., submitted to Icarus (2008)